JOURNAL OF GUIDANCE, CONTROL, AND DYNAMICS
Vol. 17, No. 4, July–August 1994

Application of Popov Controller Synthesis to Benchmark Problems with Real Parameter Uncertainty

Jonathan P. How*
Massachusetts Institute of Technology, Cambridge, Massachusetts 02139
Wassim M. Haddad†
Georgia Institute of Technology, Atlanta, Georgia 30332
and
Steven R. Hall‡
Massachusetts Institute of Technology, Cambridge, Massachusetts 02139

A new approach to robust control design with real parameter uncertainty has been developed using the analysis criteria from absolute stability theory. Both time and frequency domain stability conditions have been investigated, and the results demonstrate that the analysis tests include information about both the phase and structure of the unknown parameters. This paper uses these analysis results to investigate the synthesis of robust controllers. The control design algorithm uses state space optimization techniques to minimize an overbound of the $\mathcal{H}_2$ permormance objective that is developed using the Popov stability criterion. In this technique, the optimal compensator and multiplier coefficients are designed simultaneously, which avoids the *D-K* iteration of μ synthesis. The procedure is applied to the two and four mass benchmark problems. These examples illustrate that good guaranteed robust performance can be achieved using this Popov controller synthesis (or combined $\mathcal{H}_2$/mixed μ) algorithm.

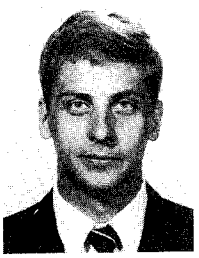

Jonathan P. How received his B.A.Sc. in Engineering Science (Aerospace Option) from the University of Toronto in 1987 and his S.M. and Ph.D. in Aeronautics and Astronautics from the Massachusetts Institute of Technology in 1990 and 1993, respectively. He is currently working as a Postdoctoral Associate on a Shuttle flight project (Middeck Active Control Experiment) in the Space Engineering Research Center at MIT. He will be joining the faculty at Stanford University as an Assistant Professor in the Department of Aeronautics and Astronautics in September, 1994. Research interests include the robust control of flexible structures and other large-scale systems. He is a Member of AIAA and IEEE.

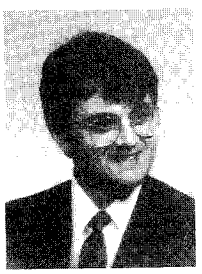

Wassim M. Haddad received the B.S., M.S., and Ph.D. degrees in mechanical engineering from the Florida Institute of Technology (FIT), Melbourne, FL, in 1983, 1984, and 1987, respectively, with specialization in dynamics and control. Since 1987, he has been a consultant for the Structural Controls Group of the Government Aerospace Systems Division, Harris Corporation. In 1988, he joined the faculty of FIT where he founded the Systems and Control option within the graduate program. His research interests are in the area of linear and nonlinear robust control. Dr. Haddad is a recipient of the National Science Foundation Presidential Faculty Fellow Award, is a member of Tau Beta Pi, and is presently an Associate Professor in the School of Aerospace Engineering at Georgia Institute of Technology.

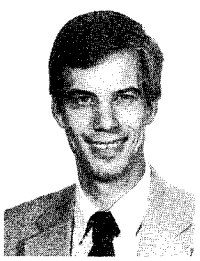

Steven R. Hall received his S.B., S.M., and Sc.D. degrees from the Massachusetts Institute of Technology Department of Aeronautics and Astronautics in 1980, 1982, and 1985, respectively. Since 1985, he has been on the faculty at the Massachusetts Institute of Technology, where he is Associate Professor of Aeronautics and Astronautics. Research interests include active control of flexible structures and the control of helicopter vibration and rotor dynamics. He is a Senior Member of AIAA, and a member of IEEE and the American Helicopter Society.

Received Nov. 3, 1992; revision received June 25, 1993; accepted for publication July 28, 1993.

Nomenclature

A, B, C	=	state space representation of $G(s)$
B_0, C_0	=	structure of the plant uncertainty
$\mathcal{E}$	=	expected value
$G(s)$	=	system transfer function
M_2, M_1	=	upper and lower sector/robustness bounds
$\mathcal{N}^r, \mathcal{D}^r, \mathcal{S}^r$	=	$r \times r$ non-negative definite, diagonal, and symmetric matrices, respectively
R_{xx}, R_{uu}, V_1, V_2	=	$\mathcal{H}_2$ weighting matrices
$W(s), H, N$	=	stability multiplier and coefficients
ΔA	=	uncertainty in the plant dynamics

I. Introduction

ONE of the most important aspects of the control design and evaluation process is the analysis of feedback systems for robust stability and performance. Significant attention has been devoted over the past several years to the use of bounded gain and other norm-based methods for these analysis tests. Unfortunately, due to their dependence on norms, these tests exclude the phase information on the system uncertainties and can be very conservative for systems with constant real parameter errors.[1-3] To reduce this conservatism, recent research has focused on improved stability criteria from the field of absolute stability theory.[1-6] The purpose of this paper is to extend these results by presenting a synthesis algorithm for controllers that guarantee robust $\mathcal{H}_2$ performance.

In many robustness techniques, such as mixed μ theory, the difficulty in directly addressing the robustness problem with real time-invariant linear uncertainties often leads to the use of approximations or upper bounds in the analysis tests.[7] These difficulties are avoided in this approach by explicitly considering the stability of a linear time-invariant system in feedback connection with an entire class of sector-bounded nonlinear functions. As a result, we can develop simpler robustness tests and provide a physical interpretation of the role of the multipliers that arise in absolute stability theory. The use of nonlinear uncertainties is an important extension of robust control for systems that exhibit nonlinear phenomena, such as spring hardening. Furthermore, as is done in this paper, these nonlinear models can be used to improve the robustness of systems with linear, constant, real parameter uncertainties.

The state space tests from absolute stability theory with Lyapunov functions of the Lur'e-Postnikov form are well documented.[5,6] However, the significance for robust control of the linearized form of these Lyapunov functions has only recently been identified.[2,4] In fact, recent work by How,[1] How and Hall,[3] and Haddad et al.[8] has demonstrated that there is a direct connection between the results of absolute stability theory from the 1960s and current work on mixed μ and K_m analysis.[9,10] This connection has largely been ignored in many of the recent developments in robust control but unifies these two diverse fields of research. Furthermore, these observations have demonstrated that the stability multipliers provide a parameterization of the μ scaling functions and that mixed μ theory is just a special case of absolute stability.[1,3,8]

As mentioned earlier, the purpose of this paper is to design robust controllers using an analysis criterion based on the Popov stability test and the Ω-bound framework developed in Refs. 2 and 11. A numerical algorithm is developed to design robust controllers that minimize an overbound of an $\mathcal{H}_2$ cost functional and satisfy an analysis test based on the Popov stability multiplier, $W(s) = I + Ns$, $N \geq 0$. The cost is simultaneously optimized with respect to the controller gains and multiplier coefficients, which avoids the iteration and curve-fitting procedures required by the *D-K* procedure of μ and K_m synthesis.[12,13] Other advantages of this new approach are that it permits the designer to prespecify the compensator order and architecture so that an optimal design with these extra conditions can be obtained. These design specifications cannot be incorporated into the standard $\mathcal{H}_\infty$ synthesis problem but are critical for most realistic systems.[14]

We proceed with a brief presentation of some mathematical preliminaries and the auxiliary minimization problem. These results are followed by an outline of the synthesis algorithm, which is then applied to two benchmark problems.

II. Mathematical Preliminaries

A. Robust Stability and Performance Problems

In the following, we present a brief outline of the robust stability and performance problems discussed in Refs. 1, 2, and 15. Let $\mathcal{U} \subset \mathcal{R}^{n \times n}$ denote a set of perturbations ΔA of a nominal matrix $A \in \mathcal{R}^{n \times n}$. The robust stability problem is to determine whether the system

$$\dot{x}(t) = (A + \Delta A)x(t) \tag{1}$$

is asymptotically stable for all $\Delta A \in \mathcal{U}$. The robust performance problem concerns the worst-case (over $\mathcal{U}$) $\mathcal{H}_2$ norm of the system

$$\dot{x}(t) = (A + \Delta A)x(t) + Dw(t) \tag{2}$$

$$z(t) = Ex(t) \tag{3}$$

where $E \in \mathcal{R}^{q \times n}$ and $w(t) \in \mathcal{R}^d$ is a zero-mean, white noise disturbance with weighting $D \in \mathcal{R}^{n \times d}$. The aim then is to determine a performance bound β satisfying

$$J(\mathcal{U}) \triangleq \sup_{\Delta A \in \mathcal{U}} \limsup_{t \to \infty} \mathcal{E}\{\|z(t)\|_2^2\} \leq \beta \tag{4}$$

We can express the $\mathcal{H}_2$ performance measure in Eq. (4) in terms of the observability Gramian for the pair $(A + \Delta A, E)$. For convenience, we define the $n \times n$ non-negative definite matrices $R \triangleq E^TE$ and $V \triangleq DD^T$.

Lemma 1.[2] Suppose $A + \Delta A$ is asymptotically stable for all $\Delta A \in \mathcal{U}$. Then

$$J(\mathcal{U}) = \sup_{\Delta A \in \mathcal{U}} \operatorname{tr} P_{\Delta A} V \tag{5}$$

where $P_{\Delta A} \in \mathcal{R}^{n \times n}$ is the unique, non-negative definite solution to

$$0 = (A + \Delta A)^T P_{\Delta A} + P_{\Delta A}(A + \Delta A) + R \tag{6}$$

Proof. See Ref. 2. □

Because D and E can be rank deficient, there may exist cases with a finite performance bound for which Eq. (1) is not asymptotically stable for all perturbations in the set $\mathcal{U}$. However, in practice, robust performance is mainly of interest when Eq. (1) is robustly stable, and our approach is to obtain robust stability as a consequence of the sufficient conditions for robust performance.

To proceed with the robust performance problem, we bound the uncertain terms $\Delta A^T P_{\Delta A} + P_{\Delta A}\Delta A$ in Eq. (6) by means of a parameter-dependent function $\Omega(P, \Delta A)$. The following result is fundamental and forms the basis for further developments.

Theorem 1.[2] Let Ω_0: $\mathcal{N}^n \to \mathcal{S}^n$ and P_0: $\mathcal{U} \to \mathcal{S}^n$ be such that

$$\Delta A^T P + P\Delta A \leq \Omega(P, \Delta A) \triangleq \Omega_0(P) - [(A + \Delta A)^T P_0(\Delta A) + P_0(\Delta A)(A + \Delta A)] \tag{7}$$

for all $\Delta A \in \mathcal{U}$ and $P \in \mathcal{N}^n$. Suppose there exists $P \in \mathcal{N}^n$ satisfying

$$0 = A^T P + PA + \Omega_0(P) + R \tag{8}$$

such that $P + P_0(\Delta A)$ is non-negative definite for all $\Delta A \in \mathcal{U}$. Then $(A + \Delta A, E)$ is detectable for all $\Delta A \in \mathcal{U}$ if, and only if, $A + \Delta A$ is asymptotically stable for all $\Delta A \in \mathcal{U}$. In this case, $P_{\Delta A} \leq P + P_0(\Delta A)$, for all $\Delta A \in \mathcal{U}$, where $P_{\Delta A}$ is given by Eq. (6). Therefore,

$$J(\mathcal{U}) \leq \operatorname{tr} PV + \sup_{\Delta A \in \mathcal{U}} \operatorname{tr} P_0(\Delta A)V \tag{9}$$

Also, if there exists $\bar{P}_0 \in \mathcal{E}^n$ such that $P_0(\Delta A) \leq \bar{P}_0$, for all $\Delta A \in \mathcal{U}$, then $J(\mathcal{U}) \leq \beta$, where $\beta \triangleq \operatorname{tr}[(P + \bar{P}_0)V]$.

Proof. See Ref. 2. □

Remark 1. If R is positive definite, then the detectability hypothesis of Theorem 1 is automatically satisfied. However, Theorem 1 can be strengthened by noting that the detectability assumption is, in a sense, superfluous. Robust stability concerns only the undisturbed system in Eq. (1), whereas R involves the $\mathcal{H}_2$ performance weighting. Hence, robust stability is guaranteed by the existence of a solution $P \in \mathcal{N}^n$ satisfying Eq. (8) with R replaced by αI_n ($\alpha > 0$) for which detectability is automatically satisfied. However, for robust performance, P in Eq. (9) must be obtained from Eq. (8).

We call $\Omega(\cdot,\cdot)$ a parameter-dependent Ω-bound, and note that the preceding framework establishing robust stability is equivalent to the existence of a parameter-dependent Lyapunov function of the form $V(x) = x^T[P + P_0(\Delta A)]x$ which also establishes robust stability.[2] For convenience in the following results we shall write $P_0(F)$ in place of $P_0(\Delta A)$.

B. Diagonal Popov Criterion

We now consider the particular case of m independent scalar parameter uncertainties. For this problem, we introduce the diagonal matrices $M_1, M_2 \in \mathcal{D}^m$, where it is assumed that $M_2 - M_1$ is positive definite. The set $\mathcal{U}$ is then defined as

$$\mathcal{U} \triangleq \{\Delta A \in \mathcal{R}^{n\times n}: \Delta A = B_0 F C_0, \text{ where } F \in \mathcal{F}\} \tag{10}$$

where $\mathcal{F}$ is given by

$$\mathcal{F} \triangleq \{F \in \mathcal{D}^m: \quad M_1 \leq F \leq M_2\} \tag{11}$$

$B_0 \in \mathcal{R}^{n\times m}$ and $C_0 \in \mathcal{R}^{m\times n}$ are fixed matrices that denote the structure of the uncertainty, and $F \in \mathcal{D}^m$ is an uncertain matrix. Note that the diagonal matrices M_2 and M_1 represent upper and lower bounds, respectively, on the elements of the uncertain diagonal matrix F.

Note that Theorem 1 provides an upper bound for the $\mathcal{H}_2$ performance for a system satisfying the conditions for robust stability for all perturbations $\mathcal{U}$ given by Eq. (10), which can be used to develop the following result.

Theorem 2. Let $M_1, M_2, N \in \mathcal{D}^m$ be such that $M_2 - M_1$ is positive definite, N is non-negative definite, and

$$R_0 \triangleq [(M_2 - M_1)^{-1} - NC_0B_0] + [(M_2 - M_1)^{-1} - NC_0B_0]^T > 0 \tag{12}$$

Furthermore, suppose there exists a non-negative definite matrix P, satisfying

$$\begin{aligned} 0 = {} & (A + B_0M_1C_0)^TP + P(A + B_0M_1C_0) + R \\ & + [C_0 + NC_0(A + B_0M_1C_0) + B_0^TP]^TR_0^{-1} \\ & \times [C_0 + NC_0(A + B_0M_1C_0) + B_0^TP] \end{aligned} \tag{13}$$

Then $(A + \Delta A, E)$ is detectable for all $\Delta A \in \mathcal{U}$ if, and only if, $A + \Delta A$ is asymptotically stable for all $\Delta A \in \mathcal{U}$. In this case,

$$J(\mathcal{U}) \leq \mathcal{J}(\mathcal{U}) \triangleq \operatorname{tr}[P + C_0^T(M_2 - M_1)NC_0]V \tag{14}$$

Proof. The proof is a direct consequence of Theorem 1 using

$$\begin{aligned} \Omega_0(P) \triangleq {} & [C_0 + NC_0(A + B_0M_1C_0) + B_0^TP]^T \\ & \times R_0^{-1}[C_0 + NC_0(A + B_0M_1C_0) + B_0^TP] \\ & + PB_0M_1C_0 + C_0^TM_1B_0^TP \end{aligned} \tag{15}$$

$$P_0(F) \triangleq C_0^T(F - M_1)NC_0 \tag{16}$$

which satisfy the conditions in Theorem 1. Because F is lower bounded by M_1 and N is non-negative definite, then $(F - M_1)N \geq 0$ for all $F \in \mathcal{F}$, and it follows that $P + P_0(F)$ is non-negative definite for all $F \in \mathcal{F}$, as required by Theorem 1. See Ref. 4 for further details. □

A geometric interpretation of the stability criterion in Theorem 2 is discussed in How and Hall.[3] The Nyquist plane test is similar to the one discussed by Hsu and Meyer[16] and can be interpreted in terms of a family of frequency dependent off-axis circles. For the case with symmetric sector bounds $M_1 = -M_2$, the location of the circle center varies along the imaginary axis as a function of the phase of the Popov multiplier, but each circle has the same real axis intercepts at $\pm M_2^{-1}$. Because the location of the circle center changes with frequency, the robustness test considers a restricted class of complex uncertainties. It follows from this result that the stability condition includes phase information about the parameter uncertainty.[1,3,8] Theorem 2 is a generalization of the classic parabola test of Ref. 17.

How and Hall[3] also demonstrate that there are very close connections between the frequency domain stability condition from absolute stability theory and upper bounds for mixed μ. In fact, it is shown that the multipliers of absolute stability theory correspond to a particular parameterization of the scaling functions in μ theory. By considering other classes of nonlinearities, How and Hall[3] and Haddad et al.[8] extend the stability criteria in Theorem 2 to include other classes of nonlinear functions. The approach can then be used for systems that have both real and complex and linear and nonlinear uncertainties, which is an extension of current robust control theory.

With the framework in Theorem 2 for overbounding the $\mathcal{H}_2$ cost for a system satisfying the multivariable Popov stability criterion, we can now complete the development of the control synthesis procedure.

III. Dynamic Output Feedback Controllers

Consider the dynamic robust stability and performance problem for the nth-order stabilizable and detectable system with constant structured real-valued plant parameter variations

$$\dot{x}(t) = (A + \Delta A)x(t) + D_1w(t) + Bu(t) \tag{17}$$

$$y(t) = Cx(t) + D_2w(t) \tag{18}$$

where $u(t) \in \mathcal{R}^{m_0}$, $w(t) \in \mathcal{R}^d$, and $y(t) \in \mathcal{R}^l$. The synthesis problem is to determine an n_cth order dynamic compensator

$$\dot{x}_c(t) = A_cx_c(t) + B_cy(t) \tag{19}$$

$$u(t) = C_cx_c(t) \tag{20}$$

that satisfies the following design criteria: 1) the closed-loop system in Eqs. (17–20) is asymptotically stable for all $\Delta A \in \mathcal{U}$; and 2) the performance functional J is minimized, where

$$J(A_c, B_c, C_c) \triangleq \sup_{\Delta A \in \mathcal{U}} \limsup_{t\to\infty} \frac{1}{t}\mathcal{E}\left\{\int_0^t [x^TR_{xx}x + u^TR_{uu}u]ds\right\} \tag{21}$$

For the uncertainties $\Delta A \in \mathcal{U}$, the closed-loop system in Eqs. (17–20) can be written as

$$\dot{\tilde{x}}(t) = (\tilde{A} + \Delta\tilde{A})\tilde{x}(t) + \tilde{D}w(t) \tag{22}$$

where

$$\tilde{x} \triangleq \begin{bmatrix} x \\ x_c \end{bmatrix}, \qquad \tilde{A} \triangleq \begin{bmatrix} A & BC_c \\ B_cC & A_c \end{bmatrix}$$
$$\Delta\tilde{A} \triangleq \begin{bmatrix} \Delta A & 0_{n\times n_c} \\ 0_{n_c\times n} & 0_{n_c\times n_c} \end{bmatrix} \tag{23}$$

Let $V_1 = D_1 D_1^T$, $V_2 = D_2 D_2^T$, and for simplicity, assume that $D_1 D_2^T = 0$. Then the closed-loop disturbance $\tilde{D}w(t)$ has intensity $\tilde{V} = \tilde{D}\tilde{D}^T$, where

$$\tilde{D} \triangleq \begin{bmatrix} D_1 \\ B_cD_2 \end{bmatrix}, \quad \text{so that} \quad \tilde{V} \triangleq \begin{bmatrix} V_1 & 0 \\ 0 & B_cV_2B_c^T \end{bmatrix} \tag{24}$$

The closed-loop system uncertainty $\Delta\tilde{A}$ in Eq. (23) has the form $\Delta\tilde{A} = \tilde{B}_0 F \tilde{C}_0$, where

$$\tilde{B}_0 \triangleq \begin{bmatrix} B_0 \\ 0_{n_c\times m} \end{bmatrix} \text{ and } \tilde{C}_0 \triangleq [C_0 \quad 0_{m\times n_c}] \tag{25}$$

Note that $\tilde{C}_0 \tilde{B}_0 = C_0 B_0$, so that

$$\begin{aligned} \tilde{R}_0 &\triangleq (M_2 - M_1)^{-1} - N\tilde{C}_0\tilde{B}_0 + [(M_2 - M_1)^{-1} - N\tilde{C}_0\tilde{B}_0]^T \\ &= (M_2 - M_1)^{-1} - NC_0B_0 + [(M_2 - M_1)^{-1} - NC_0B_0]^T \\ &= R_0 \end{aligned} \tag{26}$$

Finally, if $\tilde{A} + \Delta\tilde{A}$ is asymptotically stable for all $\Delta A \in \mathcal{U}$ and a given compensator (A_c, B_c, C_c), then the performance measure in Eq. (21) is given by

$$J(A_c, B_c, C_c) = \sup_{\Delta A \in \mathcal{U}} \operatorname{tr} \tilde{P}_{\Delta\tilde{A}} \tilde{V} \tag{27}$$

where $\tilde{P}_{\Delta\tilde{A}}$ satisfies the $(n + n_c) \times (n + n_c)$ algebraic Lyapunov equation

$$0 = (\tilde{A} + \Delta\tilde{A})^T \tilde{P}_{\Delta\tilde{A}} + \tilde{P}_{\Delta\tilde{A}}(\tilde{A} + \Delta\tilde{A}) + \tilde{R} \tag{28}$$

where

$$\tilde{R} = \begin{bmatrix} R_{zz} & 0 \\ 0 & C_c^T R_{ww} C_c \end{bmatrix} \tag{29}$$

To proceed, we consider sector-bounded nonlinear functions in ΔA, and test stability using the Popov criterion. In particular, we replace the Lyapunov Eq. (28) with the Riccati equation which guarantees that the closed-loop system is robustly stable. Then, for the dynamic output feedback problem, Theorem 2 holds with the appropriate matrices replaced with their closed-loop counterparts. For clarity, we state the following design problem.

Dynamic auxiliary minimization problem: determine the compensator (A_c, B_c, C_c) that minimizes the $\mathcal{H}_2$ overbounding cost

$$\mathcal{J}(A_c, B_c, C_c) \triangleq \operatorname{tr}[\tilde{P} + \tilde{C}_0^T(M_2 - M_1)N\tilde{C}_o]\tilde{V} \tag{30}$$

where, with $\overline{C}_0 = \tilde{C}_0 + N\tilde{C}_0(\tilde{A} + \tilde{B}_0M_1\tilde{C}_0)$, $\tilde{P} \in \mathcal{N}^{n+n_c}$ satisfies

$$\begin{aligned} 0 &= (\tilde{A} + \tilde{B}_0M_1\tilde{C}_0)^T\tilde{P} + \tilde{P}(\tilde{A} + \tilde{B}_0M_1\tilde{C}_0) \\ &\quad + \tilde{R} + [\overline{C}_0 + \tilde{B}_0^T\tilde{P}]^T R_0^{-1}[\overline{C}_0 + \tilde{B}_0^T\tilde{P}] \end{aligned} \tag{31}$$

such that (A_c, B_c, C_c) is controllable and observable, N is nonnegative definite, and $R_0 > 0$.

To proceed, we augment the cost overbound $\mathcal{J}(A_c, B_c, C_c)$ with the constraint in Eq. (31) using the Lagrange multiplier $\tilde{Q} \in \mathcal{N}^{n+n_c}$, to form $\mathcal{L}(A_c, B_c, C_c, \tilde{P}, \tilde{Q})$. We then take the gradients of $\mathcal{L}$ with respect to the free parameters in the state space representation of the controller. Note that $\partial\mathcal{L}/\partial\tilde{Q}$ recovers Eq. (31). For convenience, we partition the symmetric matrices $\tilde{P}$ and $\tilde{Q}$ as

$$\tilde{P} = \begin{bmatrix} P_{11} & P_{12} \\ P_{12}^T & P_{22} \end{bmatrix}, \qquad \tilde{Q} = \begin{bmatrix} Q_{11} & Q_{12} \\ Q_{12}^T & Q_{22} \end{bmatrix} \tag{32}$$

where $(\cdot)_{11} \in \mathcal{N}^n$ and $(\cdot)_{22} \in \mathcal{N}^{n_c}$. A similar decomposition is also used for the product $\tilde{P}\tilde{Q}$. The gradients of the Lagrangian with respect to the controller gains can be written as

$$\begin{aligned} 0 = \frac{\partial\mathcal{L}}{\partial\tilde{P}} &= [\tilde{A} + \tilde{B}_0M_1\tilde{C}_0 + \tilde{B}_0R_0^{-1}(\overline{C}_0 + \tilde{B}_0^T\tilde{P})]\tilde{Q} \\ &\quad + \tilde{Q}[\tilde{A} + \tilde{B}_0M_1\tilde{C}_0 + \tilde{B}_0R_0^{-1}(\overline{C}_0 + \tilde{B}_0^T\tilde{P})]^T + \tilde{V} \end{aligned} \tag{33}$$

$$0 = \frac{1}{2}\frac{\partial\mathcal{L}}{\partial A_c} = P_{12}^TQ_{12} + P_{22}Q_{22} = [\tilde{P}\tilde{Q}]_{22} \tag{34}$$

$$0 = \frac{1}{2}\frac{\partial\mathcal{L}}{\partial B_c} = P_{22}B_cV_2 + [\tilde{P}\tilde{Q}]_{21}C^T \tag{35}$$

$$\begin{aligned} 0 = \frac{1}{2}\frac{\partial\mathcal{L}}{\partial C_c} &= B^T(I + B_0R_0^{-1}NC_0)^T[\tilde{P}\tilde{Q}]_{12} \\ &\quad + (R_{ww} + B^TC_0^TNR_0^{-1}NC_0B)\,C_cQ_{22} \\ &\quad + B^TC_0^TNR_0^{-1}[C_0 + NC_0(A + B_0M_1C_0)]Q_{12} \end{aligned} \tag{36}$$

Haddad and Bernstein[2] use similar results to derive explicit expressions for the resulting optimal controller in terms of the solution of four coupled Riccati equations. This synthesis problem has also been extended in Refs. 1 and 8 to consider more general stability multipliers.

Note that the matrices M_1, M_2, and N, and the structure in B_0 and C_0 can be used to examine tradeoffs between performance and robustness. As shown in Refs. 1, 4, and 8, to further reduce conservatism, one can view the multiplier matrix N as a free parameter and optimize the worst case $\mathcal{H}_2$ performance bound to obtain

$$\begin{aligned} \frac{1}{2}\frac{\partial\mathcal{L}}{\partial N} &= \frac{1}{2}(M_2 - M_1)\tilde{C}_0\tilde{V}\tilde{C}_0^T + R_0^{-1}[\overline{C}_0 + \tilde{B}_0^T\tilde{P}] \\ &\quad \times \tilde{Q}\,[(\tilde{A} + \tilde{B}_0M_1\tilde{C}_0) + \tilde{B}_0\,R_0^{-1}(\overline{C}_0 + \tilde{B}_0^T\tilde{P})]^T\tilde{C}_0^T \end{aligned} \tag{37}$$

Since $N \in \mathcal{D}^m$, only the diagonal elements of $\partial\mathcal{L}/\partial N$ can be directly influenced through the optimization process.[1]

The synthesis approach developed by How[1] uses a numerical Broyden-Fletcher-Goldfarb-Shanno (BFGS) search algorithm[18,19] to solve the optimality conditions in Eqs. (31), and 33–37. There are two main steps in the solution algorithm. An inner-loop step optimizes the cost functional by solving the gradients to obtain the best current design. The inner-loop steps are performed for fixed values of the stability bounds M_1 and M_2, which are changed in the outer loop.

The inner-loop itself consists of two main parts. The first of these determines a search direction that reduces the cost functional. The second part performs a line search to determine the step size to be taken in this search direction. The purpose of the line search is to minimize the cost function in the specified direction subject to various error constraints, such as system or compensator stability. If, for a particular design, a normalization of the system gradients is below a given tolerance, then this inner-loop optimization is said to have converged to a

solution. The bounds M_1 and M_2 are then increased using a homotopy algorithm in the outer loop. The algorithm used in these examples uses the current design as an initial condition for the next inner-loop iteration.

If the inner-loop optimization fails to converge, the last increments in M_1 and M_2 are reduced. This two step iterative process is continued until the desired stability bounds M_{1f} and M_{2f} are achieved, if possible. The iteration in this design process results in a family of robust controllers which then allows an analysis of the tradeoffs between guaranteed robustness and performance.

In terms of computation, each inner-loop step requires the solution of $(n + n_c)$th-order Riccati and Lyapunov equations, which can be quite intensive. Although only low-order examples are considered in this paper, results in Refs. 1 and 20 demonstrate that, using this approach, it is possible to design full-order robust controllers for a 24th-order system with four uncertainties and a 59th-order system with 11 uncertainties. The algorithm could be improved further with a homotopy technique similar to the one used for the optimal Popov analysis problem in Ref. 21.

As discussed earlier, this numerical algorithm determines the optimal compensator gains and multiplier coefficients simultaneously, which avoids the need to iterate between controller design and optimal multiplier evaluation. Note that both controller order and architecture constraints can easily be included in the state space optimization.[22] Because of the connections to both absolute stability theory and μ analysis, this new approach to robust control design is called both Popov controller synthesis and combined $\mathcal{H}_2$/mixed μ. The following section applies the synthesis algorithm to two illustrative robust control benchmark problems.

IV. Benchmark Control Examples

In this section, we present examples of optimal robust controllers designed using this Popov synthesis algorithm. Controllers are developed for two simple systems with constant real parameter uncertainties. The low-order benchmark problems clearly demonstrate the modifications to the compensator that are required to achieve guaranteed robust stability. In How et al.,[20] the same approach is applied to more complicated examples on the Middeck Active Control Experiment.

The first problem considers a spring uncertainty for the system illustrated in Fig. 1. The second problem investigates both inertia and multivariable stiffness uncertainties (K_1 and K_3) for the system illustrated in Fig. 2. The sensitivity of the plant transfer functions to parameter variations makes both of these systems difficult challenges for robust control design.[23,24]

Both full- and reduced-order controllers are developed in this paper. The results are presented in terms of performance robustness curves for several values of the stability bounds M_1

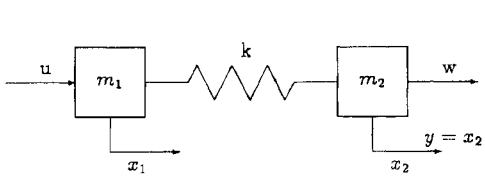

Fig. 1 Two mass oscillator.

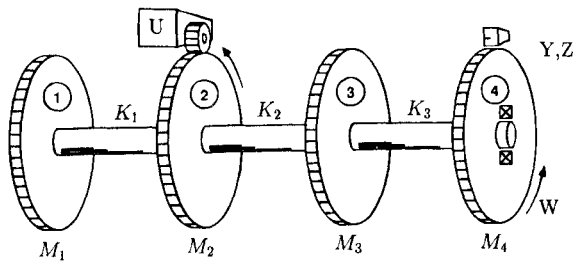

Fig. 2 Four disk oscillator.

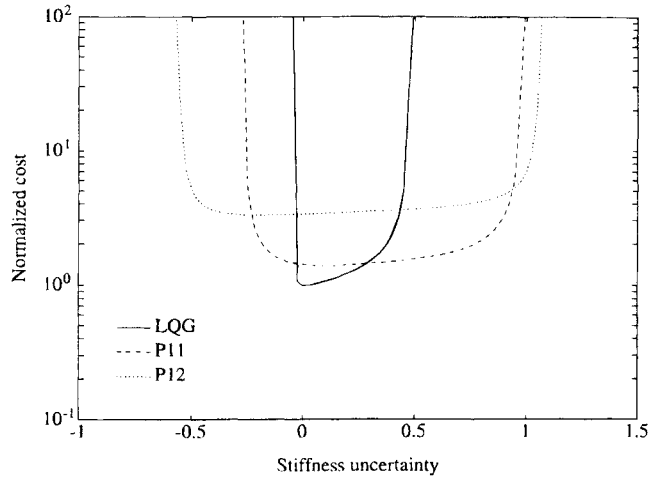

Fig. 3 Performance cost curves illustrating the tradeoff between guaranteed (and actual) robust stability and nominal/robust performance, see Table 1 for stability bounds.

and M_2. Where possible, an interpretation of how this robustness is achieved is also provided. Recall from the previous developments that M_1 and M_2 represent the guaranteed robust stability bounds, which are lower bounds on the magnitudes of the actual stability limits achieved.

A. Two Mass Spring System

Consider the two mass spring system illustrated in Fig. 1 with $m_1 = m_2 = 1$ and an uncertain spring stiffness k. A control force acts on mass 1, and a disturbance acts on mass 2. The position of mass 2 is measured, which results in a noncollocated control problem. The nominal dynamics, with the states defined in the figure, are governed by the matrices

$$A = \begin{bmatrix} 0 & 0 & 1 & 0 \\ 0 & 0 & 0 & 1 \\ -k_{\text{nom}} & k_{\text{nom}} & 0 & 0 \\ k_{\text{nom}} & -k_{\text{nom}} & 0 & 0 \end{bmatrix}, \quad B = \begin{bmatrix} 0 \\ 0 \\ 1 \\ 0 \end{bmatrix}, \quad D_1 = \begin{bmatrix} 0 & 0 \\ 0 & 0 \\ 0 & 0 \\ 1 & 0 \end{bmatrix} \tag{38}$$

$$C = [0 \quad 1 \quad 0 \quad 0], \qquad D_2 = [0 \quad 1] \tag{39}$$

where the actual spring stiffness is $k = k_{\text{nom}} + \Delta k$ and $k_{\text{nom}} = 1$. The actual dynamics of the system are given by the matrix $A_k = A + \Delta k B_0 C_0$, where $C_0 = [1 \; -1 \; 0 \; 0]$ and $\tilde{B}_0^T = [0 \; 0 \; -1 \; 1]$.

This benchmark problem is discussed in detail in Ref. 24. The example in this paper only considers design problem 1. The displacement of mass 2 was penalized, so $R_{xx} = C^T C$, $R_{uu} = \rho$, $V_2 = \rho D_2 D_2^T$, and $V_1 = D_1 D_1^T$, where $\rho = 0.001$. The goals are to achieve good nominal performance and demonstrate robust stability and performance for perturbed spring stiffness values in the range $0.5 \leq k \leq 2$.

Using the algorithm in Sec. III, several full-order ($n_c = n$) Popov compensators were designed for this uncertain system. The designs are distinguished by the labels P(a)(b), where a refers to the number of the example, and b refers to the different compensators for that example. Figure 3 compares two robust designs with the optimal linear quadratic Gaussian (LQG) controller. The graph is a plot of the $\mathcal{H}_2$ cost of the closed-loop system for various magnitudes of the parameter perturbations. In general, the system performance degrades as the magnitude of the perturbation increases. The cost curves then tend to increase, forming the characteristic "cost buckets." The cost values in this graph have been normalized with respect to the nominal LQG value to obtain J_{norm}.

The stability robustness and performance levels achieved are presented in Table 1. Note that there are no guaranteed stability robustness bounds for the LQG design. The closeness of the

actual and guaranteed stability bounds indicates that the lower stability limit is the more challenging goal to achieve. However, the results also indicate that whereas the P12 compensator guarantees stability for stiffness values in the range $(-0.4, 0.6)$, it actually achieves robust stability over the range of stiffness values specified in problem 1 of Ref. 24.

The optimal Popov (P12) and Linear Quadratic Gaussian (LQG) controllers are compared in Fig. 4 and Table 2. Although similar at high frequencies, the transfer functions of the compensators are strikingly different for frequency values near the uncertain mode. The more lightly damped nonminimum phase zero in the Popov compensator at 0.9 rad/s phase stabilizes the system for negative values of Δk. Similarly, the phase of the Popov compensator is higher at high frequencies, leading to a stable system for larger positive values of Δk. A comparison of the modifications required in the Popov compensator at high and low frequencies clearly illustrates why the lower stability limit presents the more difficult design challenge.

The transfer functions in Fig. 4 indicate that the LQG and Popov controller gains are similar in magnitude. In fact, impulse responses of the nominal and perturbed closed-loop system dynamics indicate that the Popov controllers achieve good robust performance without large increases in the controller effort.

The robustness of the two compensator designs can be compared further in terms of the gain and phase margins of the loop transfer functions. With the LQG compensator, the phase margin at 0.98 rad/s is only 4 deg and gain margin at 1.00 rad/s is only 1.06. With the Popov compensator, the phase margin at 2.02 rad/s is 37 deg and the gain margin at 3.53 rad/s is 2.5.

Table 1 Closed-loop robust performance for the two mass system with spring uncertainty, optimal multiplier for P12 is $W_{opt}(s) = 1 + 0.33s$

		Lower bound		Upper bound	
Fig. 3 label	J_{norm}	Actual	Guaranteed	Guaranteed	Actual
LQG	1.00	−0.03	0	0	0.45
P11	1.42	−0.25	−0.10	0.30	0.95
P12	3.34	−0.55	−0.40	0.60	1.05

Table 2 Comparison of LQG and P12 compensators for the two mass system, transfer functions are shown Fig. 4

Compensator	DC Gain	Poles	Zeros
		$-1.76 \pm 4.26J$	−0.65
LQG	−1.28	$-4.98 \pm 3.42J$	$0.15 \pm 1.23J$
		$-7.16 \pm 0.88J$	−0.29
P12	−0.36	$-3.63 \pm 6.23J$	$0.04 \pm 0.93J$

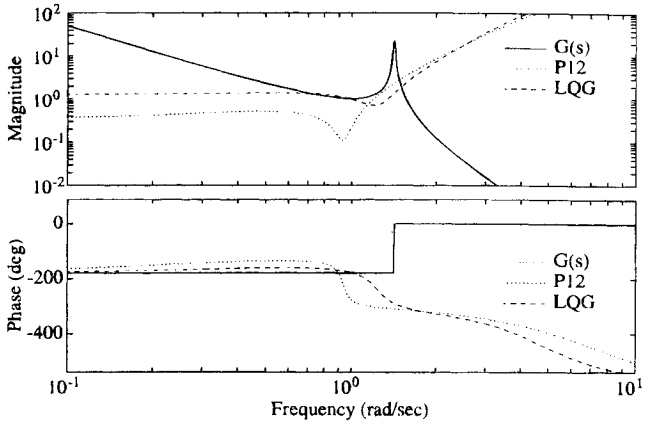

Fig. 4 Comparison of LQG and P12 compensators for the two mass system, poles and zeros given in Table 2.

We can also investigate the robustness of this simple system with one uncertainty using the Nyquist stability criterion. Consider the robust performance problem in Fig. 5. We then form the closed-loop system $M(s)$ using representations of the plant $G(s)$ and the compensator $G_c(s)$. Using a representation of $M(s)$, we can then plot the transfer function T_{rd} across the block Δ and use the Nyquist criterion to determine the values of $\Delta(s)$ that result in an unstable closed-loop system. These values are given by Δ for which $1 - T_{rd}\Delta = 0$, or equivalently, $\Delta = 1/T_{rd}$.

In Fig. 6, we plot $T_{rd}(s)$ with both the LQG and Popov (P12) controllers. Note that these curves include both magnitude and phase information about the uncertainty that leads to instability. In particular, the real-axis intercepts can be used to determine the real parameter uncertainty that can be tolerated by the system. The large negative real-axis intercept with the LQG controller corresponds to the small negative stability bound in Fig. 3. As expected, the Popov design results in a significant improvement in the magnitudes of the real-axis intercepts without substantially reducing the positive imaginary-axis intercept. Because the Popov analysis test distinguishes between real and imaginary values of the uncertainty, the approach avoids just reducing the magnitude of the entire transfer function to achieve robustness, as would be necessary with a standard small-gain type test. Also note that the shape of the transfer function with the Popov controller clearly illustrates the influence of the off-axis circle tests analyzed in Refs. 1 and 3. The transfer function with the P12 controller also indicates that extending the synthesis to more general multipliers should further reduce the conservatism for systems with real parameter uncertainty.

The results of this simple example illustrate that the Popov synthesis technique yields controllers that achieve good guaranteed robust performance. The following section applies the design approach to the more complicated system in Fig. 2.

B. Coupled Rotating Disk System

A model of the four disk system illustrated in Fig. 2, with states associated with the angular positions of each disk, is given by the matrices

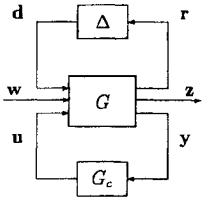

Fig. 5 Elements of the robust performance problem.

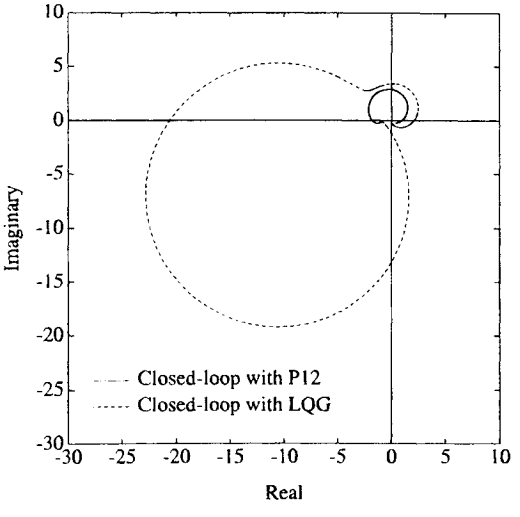

Fig. 6 Nyquist plots of the closed-loop transfer functions T_{rd} across the block Δ with both LQG and Popov (P12) controllers.

$$A = \begin{bmatrix} 0 & I \\ -M^{-1}K & -M^{-1}D \end{bmatrix}$$

$$M = m \begin{bmatrix} 0.5 & 0 & 0 & 0 \\ 0 & 1 & 0 & 0 \\ 0 & 0 & 1 & 0 \\ 0 & 0 & 0 & 1 \end{bmatrix} \tag{40}$$

$$T = \begin{bmatrix} 1 & -1 & 0 & 0 \\ -1 & 2 & -1 & 0 \\ 0 & -1 & 2 & -1 \\ 0 & 0 & -1 & 1 \end{bmatrix}$$

where $K = kT$, $D = dT$, and

$$B^T = \begin{bmatrix} 0\,0\,0\,0\,0\,(1/m)\,0\,0 \end{bmatrix}, \quad C = [0\,0\,0\,1\,0\,0\,0\,0] \tag{41}$$

$$D_1^T = \begin{bmatrix} 0 & 0 & 0 & 0 & 0 & 0 & 0 & (1/m) \\ 0 & 0 & 0 & 0 & 0 & 0 & 0 & 0 \end{bmatrix}$$
$$D_2 = [0 \quad 1] \tag{42}$$

For this model we selected $m = k = 1$, and a low damping value $d = 0.01$. The first problem considers uncertainty in the inertia of disk 1 (m_1). The second part of the problem considers independent uncertainties in the stiffness values of the springs k_1 and k_3. To complete the noise and performance specifications for the $\mathcal{H}_2$ synthesis, we define $R_{xx} = C_1^T C_1$, $R_{uu} = \rho$, $V_2 = \rho D_2 D_2^T$, and $V_1 = D_1 D_1^T$, where $\rho = 0.005$ and $C_1 = [0\,0\,0\,1\,0\,0\,0\,0.1]$.

The mass parameter uncertainty enters the system dynamics through its inverse. Thus, we will use the inverse $\tilde{m} = 1/m_1$ as the uncertain parameter. The system uncertainty is then written as

$$1/m_1 = 1/m_{\text{nom}} + \tilde{m}, \qquad m_{\text{nom}} = 0.5 \tag{43}$$

Hence, as m_1 varies from 1 to 0.25, $\tilde{m}$ varies from -1 to 2. The uncertainty in the dynamics matrix A can then be represented as $\Delta A = \tilde{m} B_0 C_0$, where

$$B_0^T = [0\,0\,0\,0\,1\,0\,0\,0]$$
$$C_0 = [-k \;\; k \;\; 0 \;\; 0 \;\; -d \;\; d \;\; 0 \;\; 0] \tag{44}$$

The robustness results with three Popov controllers are presented in Fig. 7 and Table 3. The synthesis sequence was terminated with guaranteed bounds of ± 0.16, but the actual stability limits are $-0.22 < \tilde{m} < 0.34$. These actual limits correspond to inertia values in the range $0.43 < m_1 < 0.56$. This range represents a significant fraction of the change in $m_1 (\approx 0.38)$ required to exchange the order of the poles and zeros in the open-loop system. The penalty for these robustness guarantees, in terms of performance degradation, is evident from the J_{norm} values in Table 3.

Table 3 Closed-loop robust performance with inertia uncertainty in disk 1

		Lower bound		Upper bound	
Fig. 7 label	J_{norm}	Actual	Guaranteed	Guaranteed	Actual
LQG	1.00	−0.009	0	0	0.041
P21	1.32	−0.110	−0.089	0.021	0.151
P22	1.58	−0.160	−0.115	0.115	0.250
P23	1.80	−0.220	−0.159	0.159	0.340

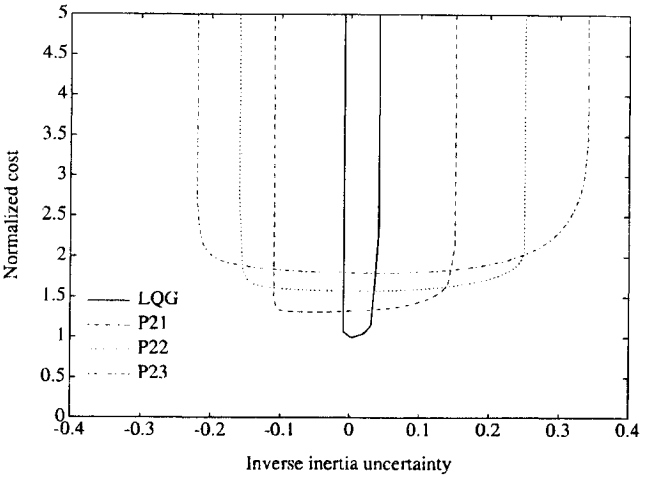

Fig. 7 Closed-loop robust stability and performance with inertia uncertainty in disk 1, see Table 3 for stability bounds.

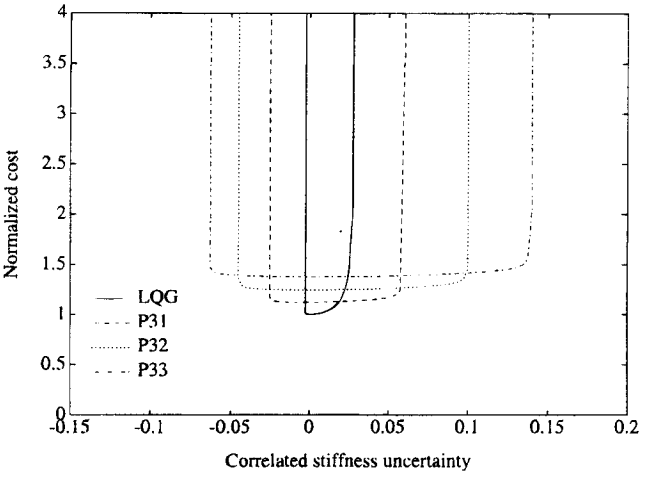

Fig. 8 Closed-loop robust stability and performance with two stiffness uncertainties; $\Delta K_1 = \Delta K_3$ assumed for the analysis; see Table 4 for stability bounds.

The second problem considers multivariable uncertainty in the stiffness values K_1 and K_3. Note that the performance of this system is dominated by the two lower frequency modes which are essentially unchanged by the model uncertainty. However, the two higher frequency modes and the zero at 1.4 rad/s are strongly influenced by the parameter uncertainty. In fact, small changes in the two stiffness values (5%) result in very large phase variations in the frequency response of the system. As a result, this benchmark problem captures many of the important features for robust control design of more complicated structures.[25]

For this problem, the uncertainty in the dynamics matrix A is written as $\Delta A = B_0 \Delta K C_0$, where

$$B_0^T = \begin{bmatrix} 0 & 0 & 0 & 0 & -2 & 1 & 0 & 0 \\ 0 & 0 & 0 & 0 & 0 & 0 & -1 & -1 \end{bmatrix}$$

$$C_0 = \begin{bmatrix} 1 & -1 & 0 & 0 & 0 & 0 & 0 & 0 \\ 0 & 0 & 1 & -1 & 0 & 0 & 0 & 0 \end{bmatrix}$$

and $\Delta K = \text{diag}(\Delta K_1, \Delta K_3)$. A more general Popov multiplier of the form $H + N_s$, ($H, N \in \mathcal{D}^2$, $H > 0$, $N \geq 0$) was used for this multivariable example.[1,15] From the discussion in Sec. III, the worst case $\mathcal{H}_2$ performance can also be optimized with respect to the diagonal elements of H.As before, several robust controllers were designed to analyze the tradeoffs between per-

formance and robustness. The optimal multiplier for the Popov P33 controller is

$$W_{\text{opt}}(s) = \begin{bmatrix} 1.00 & 0 \\ 0 & 2.57 \end{bmatrix} + \begin{bmatrix} 0.45 & 0 \\ 0 & 1.11 \end{bmatrix} s \qquad (45)$$

A comparison of the multipliers for this family of Popov compensators indicates that H and N change significantly as $M_2 = -M_1$ is increased. These changes in turn demonstrate the importance of allowing the multipliers to vary in the synthesis of the robust controllers.

Whereas the synthesis process treats multiple uncertainties as uncorrelated, for simplicity in the presentation of the results, only the case with $\Delta K_1 = \Delta K_3$ is analyzed here. The robust stability and performance results are presented in Fig. 8 and Table 4. The P33 compensator guarantees stability for 5% independent variations in the stiffness values, which represents a significant improvement over the values that the LQG design actually achieves. For this lightly damped system, these perturbations correspond to approximately ±100-deg phase variations in the plant transfer functions.

As before, there typically is a "stiff" uncertainty direction that is more difficult than the other directions. In this case, the negative uncertainty values are more difficult to achieve in this example, as can be seen by the closeness of the guaranteed and actual lower bounds in Table 4. This knowledge of a more difficult direction could be used to refine the stability bounds and accentuate the robustness for negative uncertainties. Although the discrepancy in the guaranteed and actual upper bounds is, to some extent, a measure of the conservatism in the technique, it is also a reflection of the relative ease of robustifying the system to this particular direction of the uncertainty.

The transfer functions of the optimal LQG and P33 compensators are compared in Fig. 9. The uncertainty in the zero-pole combination at approximately 1.4 rad/s and the pole at 1.9 rad/s is reflected in the Popov compensator by lower controller gains and much smoother phase. Further comparisons of the LQG and Popov designs are given in Figs. 10 and 11. The figures show the open-loop and closed-loop pole locations of the system as a function of the uncertainty $\Delta K = \Delta K_1 = \Delta K_3$ for $-0.2 \le \Delta K \le 0.2$. The LQG and P33 designs from Table 4 are compared in these figures. The two sets of closed-loop poles are plotted for the same values of Δk. The graphs also indicate the nominal closed-loop pole locations. If applicable, the pole locations at the guaranteed stability limits are also identified.

With the LQG compensator in Fig. 10, there are nominally two closed-loop poles at approximately 1.4 rad/s, the frequency of the plant zero. Further analysis of Fig. 10 indicates that the more lightly damped of these two pole pairs is extremely sensitive to changes in the stiffness values. It is well known that high-performance LQG controllers tend to invert the system dynamics, which results in high gains at system zeros and compensator zeros at plant poles. The resulting controllers are then extremely sensitive to variations in the frequencies of these poles and zeros.

A similar examination of the closed-loop poles with the Popov compensator in Fig. 11 indicates that several key changes have occurred. Consider the four poles closest to the imaginary axis. Compared with the LQG design, the three lower frequency ones are more heavily damped, but the highest frequency one is essentially unchanged. The improved robustness of the closed-loop system to stiffness uncertainty is clearly evident by comparing the root loci in Fig. 11 with those in Fig. 10. In particular, note that in the Popov design, the compensator poles

Table 4 Robust stability and performance for the closed-loop system with two stiffness uncertainties, $\Delta K_1 = \Delta K_3$ assumed for the analysis

		Lower bound		Upper bound	
Fig. 8 label	J_{norm}	Actual	Guaranteed	Guaranteed	Actual
LQG	1.00	−0.003	0	0	0.028
P31	1.12	−0.025	−0.019	0.019	0.060
P32	1.25	−0.045	−0.035	0.035	0.100
P33	1.38	−0.063	−0.051	0.051	0.140

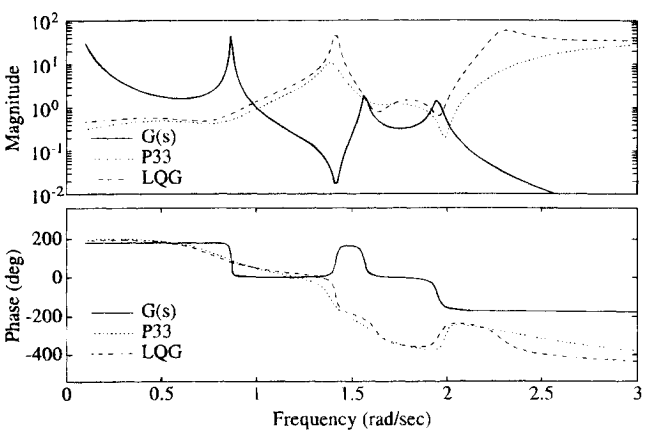

Fig. 9 Optimal LQG and P33 compensator comparison for the system $G(s)$ with two stiffness uncertainties.

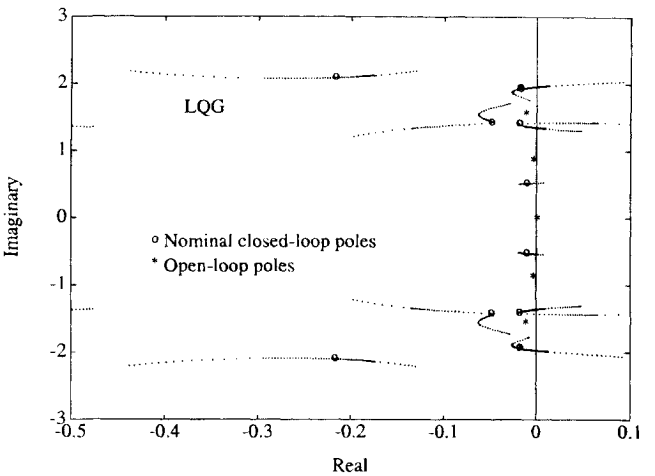

Fig. 10 Closed-loop pole locations with the LQG compensator for $\Delta K = \Delta K_1 = \Delta K_3$ and $-0.2 \le \Delta K \le 0.2$.

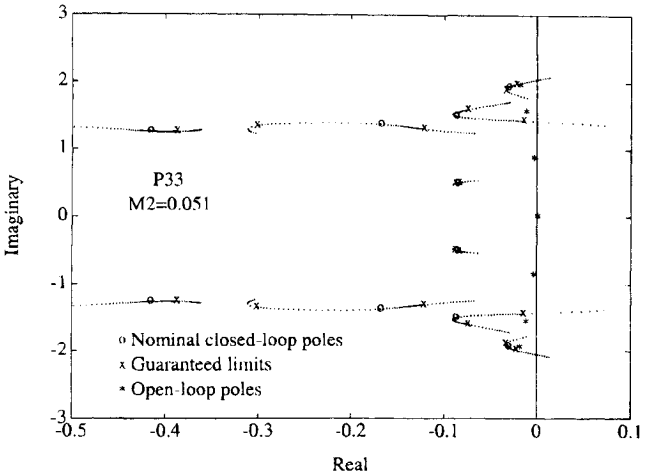

Fig. 11 Closed-loop pole locations with the P33 compensator for $\Delta K = \Delta K_1 = \Delta K_3$ and $-0.2 \le \Delta K \le 0.2$.

Table 5 Closed-loop robust stability and performance with two stiffness uncertainties, comparison of full- (P41) and reduced-order (P42) designs, $\Delta k_1 = \Delta k_3$ assumed for the analysis

		Lower bound		Upper bound	
Fig. 12 label	J_{norm}	Actual	Guaranteed	Guaranteed	Actual
LQG	1.00	−0.003	0	0	0.028
P41	1.17	−0.033	−0.024	0.024	0.075
P42	1.27	−0.035	−0.025	0.025	0.200

Table 6 Comparison of a full- (P41) and reduced-order (P42) Popov compensator for the system with two stiffness uncertainties, stability boundaries are provided in Table 5

Design	DC Gain	Poles	Zeros
		$-0.02 \pm 1.40J$	−0.26
		$-0.31 \pm 2.35J$	$0.17 \pm 0.80J$
P41	−0.36	$-2.18 \pm 1.51J$	$0.08 \pm 1.60J$
		$-2.41 \pm 2.85J$	$-0.03 \pm 1.97J$
		$-0.02 \pm 1.40J$	−0.27
P42	−0.34	$-0.85 \pm 0.98J$	$0.17 \pm 0.83J$
		$-2.03 \pm 7.15J$	$-0.06 \pm 1.65J$

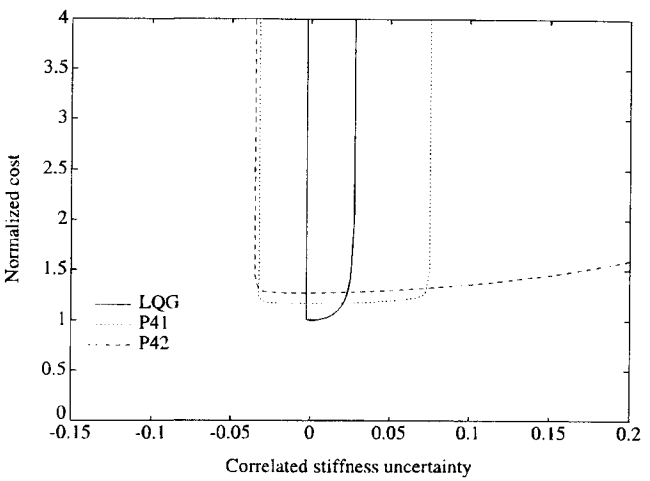

Fig. 12 Closed-loop robust stability and performance with two stiffness uncertainties, compares full and reduced-order designs; see Table 5 for the corresponding stability bounds.

at approximately 1.4 rad/s are shifted away from the plant zero. The approach then avoids the pole-zero cancellations in the closed-loop system that lead to such sensitive LQG designs. The traces in Fig. 11 also indicate that additional robustness is achieved by changing the departure angle of the closed-loop poles when plotted vs the uncertain parameter ΔK.

The last part of this problem considers the design of a reduced-order Popov controller ($n_c = 6$) for the system with multiple stiffness uncertainties. The stability robustness and performance values for the full-order (P41) and reduced-order (P42) designs are given in Fig. 12 and Table 5. Because the optimal compensator order is $n_c = n = 8$, the nominal performance of this suboptimal design ($n_c = 6 < n$) is expected to be worse than both the LQG and full-order Popov designs. This is clearly evident in the table by the larger value of J_{norm}. Although Fig. 12 apparently indicates that the reduced-order design is more robust to increases in the stiffness values, this conclusion may not be valid for other combinations of ΔK_1 and ΔK_3.

The poles and zeros of the full- and reduced-order controllers are compared in Table 6. The results indicate that the controllers are quite similar up to approximately 1.5 rad/s. However, the two designs differ at higher frequencies due to the reduced number of compensator poles and zeros. The reduced-order design loses a pole in the 2.5–3.5-rad/s range and the zero at 2 rad/s. The loss of the phase recovery associated with this zero is accounted for in the reduced-order design by moving the highest frequency pole pair to approximately 7 rad/s.

V. Conclusions

The results from these examples illustrate the capabilities of Popov controller synthesis for robust control design with constant real parameter uncertainty. The robust performance curves clearly illustrate the tradeoffs between guaranteed stability and $\mathcal{H}_2$ performance. The relative flatness of the cost curves indicates that similar performance levels will be achieved for all parameter variations in the ranges of guaranteed and actual stability.

The importance of these benchmark problems is that one can easily identify the modifications to the compensator required to achieve the guaranteed robustness. However, recent results have demonstrated that this Popov controller synthesis or combined $\mathcal{H}_2$/mixed μ approach to robust control is feasible for more realistic systems such as the Middeck Active Control Experiment.

Acknowledgments

The research was funded in part by the National Science Foundation NSF Grant ECS-9109558, NASA Grant NAGW-2014, and NASA SERC Grant NAGW-1335. The authors would like to thank Harris Corporation for providing Fig. 2.

References

[1] How, J. P., "Robust Control Design with Real Parameter Uncertainty using Absolute Stability Theory," Ph.D. Thesis, Department of Aeronautics and Astronautics, Massachusetts Inst. of Technology, Cambridge, MA, MIT SERC Rept. 1–93, Feb. 1993.

[2] Haddad, W. M., and Bernstein, D. S., "Parameter-Dependent Lyapunov Functions, Constant Real Parameter Uncertainty, and the Popov Criterion in Robust Analysis and Synthesis, Parts I and II," *Proceedings of the IEEE Conference on Decision and Control*, IEEE, Piscataway, NJ, 1991, pp. 2274–2279, 2632–2633.

[3] How, J. P., and Hall, S. R., "Connections between the Popov Stability Criterion and Bounds for Real Parameter Uncertainty," *Proceedings of the American Control Conference* (San Francisco, CA), Inst. of Electrical and Electronics Engineers, Piscataway, NJ, June 1993, pp. 1084–1089.

[4] Haddad, W. M., and Bernstein, D. S.,"The Multivariable Parabola Criterion for Robust Controller Synthesis: A Riccati Equation Approach," Journal of Mathematics, Systems, Estimation, and Control, to be published.

[5] Popov, V. M., "On Absolute Stability of Non-linear Automatic Control Systems," *Automatika I Telemekhanika*, Vol. 22, No. 8, 1961, pp. 961–979.

[6] Narendra, K. S., and Taylor, J. H., *Frequency Domain Criteria for Absolute Stability*, Academic Press, New York, 1973.

[7] Fan, M. K. H., Tits, A. L., and Doyle, J. C., "Robustness in the Presence of Mixed Parametric Uncertainty and Unmodelled Dynamics," *IEEE Transactions on Automatic Control*, Vol. AC-36, No. 1, 1991, pp. 25–38.

[8] Haddad, W. M., How, J. P., Hall, S. R., and Bernstein, D. S., "Extensions of Mixed-μ Bounds to Monotonic and Odd Monotonic Nonlinearities Using Absolute Stability Theory," *Proceedings of the IEEE Conference on Decision and Control* (Tucson, AZ), IEEE, Piscataway, NJ, 1992, pp. 2713–2819, 2820–2823; *International Journal of Control*, (submitted for publication).

[9] Young, P. M., Newlin, M. P., and Doyle, J. C., "μ Analysis with Real Parametric Uncertainty," *Proceedings of the IEEE Conference on Decision and Control* (Brighton, England, UK), IEEE, Piscataway, NJ, 1991, pp. 1251–1256.

[10] Safonov, M. G., and Chiang, R. Y., "Real/Complex K_m-Synthesis without Curve Fitting," *Control and Dynamic Systems*, Vol. 56, Part 2, Academic Press, New York, 1993, pp. 303–324.

[11] Bernstein, D. S., and Hyland, D. C., "The Optimal Projection Approach to Robust, Fixed-Structure Control Design," *Mechanics and Control of Space Structures* edited by J. L. Junkins, AIAA, Washington, DC, 1990, pp. 237–293.

[12] MuSyn Inc., *μ-Analysis and Synthesis Tollbox: User's Guide*, Math Works, Inc., Natick, MA, 1991.

[13] Safonov, M. G., and Lee, P. H., "A Multiplier Method for Computing Real Multivariable Stability Margin," July 1993, presented at the *IFAC World Congress*, Sydney, Australia.

[14] Miller, D., Saarmaa, E., and Jacques, R., "Preliminary Structural Control Results From the Middeck Active Control Experiment (MACE)," *AIAA Dynamics Specialist Conference* (Dallas, TX), AIAA, Washington DC, 1992, pp. 566–576; (AIAA Paper-92-2138).

[15] How, J. P., Haddad, W. M., and Hall, S. R., "Robust Control Synthesis Examples with Real Parameter Uncertainty using the Popov Criterion," *Proceedings of the American Control Conference* (San Francisco, CA), Inst. of Electrical and Electronics Engineers, Piscataway, NJ, 1993, pp. 1090–1095.

[16] Hsu, J. C., and Meyer, A. U., *Modern Control Principles and Applications*, McGraw-Hill, New York, 1968.

[17] Bergen, A. R., and Sapiro, M. A., "The Parabola Test for Absolute Stability," *IEEE Transactions on Automatic Control*, June 1967, pp. 312–314.

[18] Scales, L. E., *Introduction to Non-Linear Optimization*, Springer-Verlag, New York, 1985.

[19] Shanno, D. F., and Phua, K. H., "Minimization of Unconstrained Multivariable Functions," *ACM Trans. Math. Appl.*, Vol. 6, 1980, pp. 618–622.

[20] How, J. P., Hall, S. R., and Haddad, W. M., "Robust Controllers for the Middeck Active Control Experiment using Popov Controller Synthesis," *IEEE Transactions on Control Systems Technology*, (submitted for publication). AIAA Guidance, Navigation, and Control Conference, Aug. 1993, pp. 1611–1621.

[21] Collins, E. G., Jr., Haddad, W. M., and Davis, L. D., "Riccati Equation Approaches for Robust Stability and Performance Analysis Using the Small Gain, Positivity, and Popov Theorems," *Journal of Guidance, Control, and Dynamics*, Vol. 17, No. 2, 1994, pp. 322–329.

[22] Mercadal, M., "$\mathcal{H}_2$ Fixed Architecture, Control Design for Large Scale Systems," Ph.D. Thesis, Department of Aeronautics and Astronautics, Massachusetts Inst. of Technology, Cambridge, MA, June 1990.

[23] Cannon, R. H., and Rosenthal, D. E., "Experiments in Control of Flexible Structures with Noncolocated Sensors and Actuators," *Journal of Guidance, Control, and Dynamics*, Vol. 7, No. 5, 1984, pp. 546–553.

[24] Wie, B., and Bernstein, D. S., "Benchmark Problems for Robust Control Design," *Journal of Guidance, Control, and Dynamics*, Vol. 15, No. 5, 1992, pp. 1057–1059.

[25] Junkins, J. L., *Mechanics and Control of Space Structures*, AIAA, Washington, DC.